JTE HCMUTE
ISSN: 2615-9740
JOURNAL OF TECHNICAL EDUCATION SCIENCE
Ho Chi Minh City University of Technology and Education
Website: https://jte.edu.vn
Email: jte@hcmute.edu.vn

Enhanced-Mode NiO/β-Ga_2O_3 Heterojunction Field-Effect Transistor: A TCAD Study

Duc-Minh Truong, Ngoc-Hung Nguyen, Huy-Binh Do*
Ho Chi Minh City University of Technology and Education, Vietnam

**Corresponding author. Email: binhdh@hcmute.edu.vn*

ARTICLE INFO

Received:	06/10/2024
Revised:	15/10/2024
Accepted:	23/10/2024
Published:	28/11/2025

KEYWORDS

Ga_2O_3;

NiO;

NiO/Ga_2O_3 p-n junction;

MOSFETs;

Power devices.

ABSTRACT

Ga_2O_3 is considered to be a promising candidate for the fabrication of high-power semiconductor devices because it has the wide range of band gap from 3.0 eV to 4.9 eV. Because the lack of p-type Ga_2O_3, p-type NiO/n-type Ga_2O_3 MOSFETs is expected to realize Ga_2O_3 power MOSFETs in industry because both Ga_2O_3 and NiO have wide band gap and high critical electric field. In this work, p-type NiO/n-type Ga_2O_3 MOSFETs were investigated under the effects of gate-drain distance L_{GD} and acceptor concentration N_A in NiO layer, using TCAD simulations. It was found that drain current increases 3 times as the L_{GD} decreases in a range from 8 µm to 1 µm. N_A of NiO layer strongly affects the threshold voltage V_{th} of the devices, illustrating the positive shift of V_{th} as N_A increased from 1.0×10^{16} cm^{-3} to 1.0×10^{20} cm^{-3}. The NiO/Ga_2O_3 MOSFETs operates in E-mode with $V_{th} > 0$ when $N_A \geq 1.0\times10^{18}$ cm^{-3}. The change in N_A leads to the transformation of NiO/Ga_2O_3 junction, from a linear-junction ($N_A = 1.0\times10^{16}$ cm^{-3}) to an abrupt-junction ($N_A = 1.0\times10^{20}$ cm^{-3}). The rise in Schottky barrier within the depletion region at NiO/Ga_2O_3 junction creates the E-mode of the p-type NiO/n-type Ga_2O_3 MOSFETs.

Doi: https://doi.org/10.54644/jte.2025.1665

Copyright © JTE. This is an open access article distributed under the terms and conditions of the Creative Commons Attribution-NonCommercial 4.0 International License which permits unrestricted use, distribution, and reproduction in any medium for non-commercial purpose, provided the original work is properly cited.

1. Introduction

β-Ga_2O_3 has been considered as a potential wide bandgap semiconductor for several applications such as UV photodetectors, photocatalysts, gas sensors, solar cells, and power devices [1], [2]. β-Ga_2O_3 posed ultra-wide band-gap (4.6 - 4.9 eV) with high critical electric field of 8 MV/cm, inducing a high Baliga's figure of merit (BFOM) of 3444 which is potential for high power electronic applications [3]. The substrates of β-Ga_2O_3 can be produced by low-cost methods such as Czochralski (CZ), floating zone (FZ) and edge-defined film-fed growth (EFG) [4], [5], making it a superior option for high power applications comparing to other wide bandgap materials such as SiC and GaN. The epitaxial β-Ga_2O_3 films can be grown with manageable n-type doping by using flexible methods such as metalorganic chemical vapor deposition (MOCVD), molecular beam epitaxy (MBE), and halide vapor phase epitaxy (HVPE), making a fact that the design and fabrication of β-Ga_2O_3 devices are cost-effective and controllable [6]-[8].

Although abundant studies of β-Ga_2O_3 devices has been conducted [9], [10], realizing β-Ga_2O_3 devices in industry still encounters two major challenges [11]: (1) the low thermal conductivity of β-Ga_2O_3 film and (2) the lack of method to growth p-type β-Ga_2O_3 films. To improve heat dissipation of β-Ga_2O_3 film which induces the self-heating in β-Ga_2O_3 devices, the flip-chip package integrated with the heat sink is considered to be an effective method. So, p-type β-Ga_2O_3 seems to be the main obstacle that hinders the realization of β-Ga_2O_3 devices. Several methods have been adapted to investigate the normally-off β-Ga_2O_3 metal oxide semiconductor field effect transistors (MOSFETs), including fin structure [12], ferroelectric dielectric [13], gate work function modulation [14], recessed-gate MOSFETs [15], nitrogen doping [16], and oxygen annealing [17]. Do et al. has used recessed-gate β-Ga_2O_3/semi-insulator Fe-doped Ga_2O_3 to achieve enhanced-mode (E-mode) MOSFETs [15]. However, high densities of defects in Fe-doped Ga_2O_3 substrates may lead to reduce charge density in the β-Ga_2O_3 channel when its thickness is small, causing large on-resistances and enormous conduction losses.

JTE HCMUTE
ISSN: 2615-9740
JOURNAL OF TECHNICAL EDUCATION SCIENCE
Ho Chi Minh City University of Technology and Education
Website: https://jte.edu.vn
Email: jte@hcmute.edu.vn

Recently, Nickel oxide (NiO) has risen as an emerging wide bandgap p-type semiconductor (band gap ~ 3.8 eV) which can be integrated with Ga_2O_3 power device to achieve E-mode NiO/ Ga_2O_3 MOSFETs, due to the decent hole mobility, wide range of doping of NiO [18]. The advantage of NiO is that it can be grown and doped flexibly using popular deposition technology such as radio frequency magnetron sputtering (RF sputtering) [19]. There have been several reports that p-NiO/n-Ga_2O_3 heterojunction was used to fabricate power diode and FET [20]-[22], showing high values of BFOM and high break down voltage. However, the study of the effects of gate-drain distance and the concentration of p-type NiO on E-mode p-NiO/n-Ga_2O_3 MOSFETs has not been conducted systematically.

This study arms to design and investigate the impacts of n-type Ga_2O_3 gate-drain distance and the doping concentration of p-type NiO substrate on the properties of p-NiO/n-Ga_2O_3 MOSFETs. Before investigating the properties of p-NiO/n-Ga_2O_3 MOSFETs, a calibration of p-NiO/n-Ga_2O_3 junction was conducted using structure shown in Fig. 1 to ensure that the simulation parameters are reliable. The calibration was made by comparing the simulated I-V curve with experimental ones. The band diagram of p-NiO/n-Ga_2O_3 MOSFETs are investigated to find out which factors that affect the threshold voltage of p-NiO/n-Ga_2O_3 MOSFETs. Al_2O_3 is chosen as a high-k layer for p-NiO/n-Ga_2O_3 MOSFETs because it has high permittivity of 10 and low interface trap density of 5×10^{11} cm^{-2} eV^{-1} at Al_2O_3/Ga_2O_3 interface [23].

2. Simulation details

Table 1. *The details of material parameters of Ga_2O_3 and NiO used in the simulation*

Parameters	n-type Ga_2O_3 [15]	p-type NiO [24]
Band Gap (eV)	4.8	4.5
Electron Affinity (eV)	4.0	1.9
Effective electron mass	0.28	0.20
Relative dielectric constant	11	10.7
Room-temperature electron mobility (cm^2/Vs)	130	-
Room-temperature hole mobility (cm^2/Vs)	-	0.12
Saturation electron velocity (cm/s)	2.00×10^7	-
Saturation hole velocity (cm/s)	-	1.91×10^7

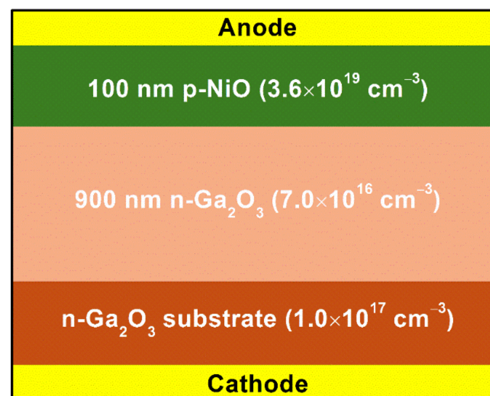

Figure 1. *Schematic cross section of NiO/β-Ga_2O_3 p-n junction diode.*

JTE
HCMUTE
ISSN: 2615-9740

JOURNAL OF TECHNICAL EDUCATION SCIENCE
Ho Chi Minh City University of Technology and Education
Website: https://jte.edu.vn
Email: jte@hcmute.edu.vn

The p-type NiO/n-type Ga_2O_3 p-n junction was studied using the 2-D device simulation tool to calibrate the simulation parameters. The device structure is illustrated in Fig. 1. The simulated parameters of Ga_2O_3 and NiO are shown in Table 1. A concentration-dependent lifetime model and a high field model were adapted to consider the effects of carrier concentration and high electrical field on the mobility of Ga_2O_3 and NiO layers. For the recombination and generation in Ga_2O_3 and NiO layers, the Auger recombination model was utilized. The thermal model was used in this study to inspect the self-heating effect in the devices.

3. Results and Discussion

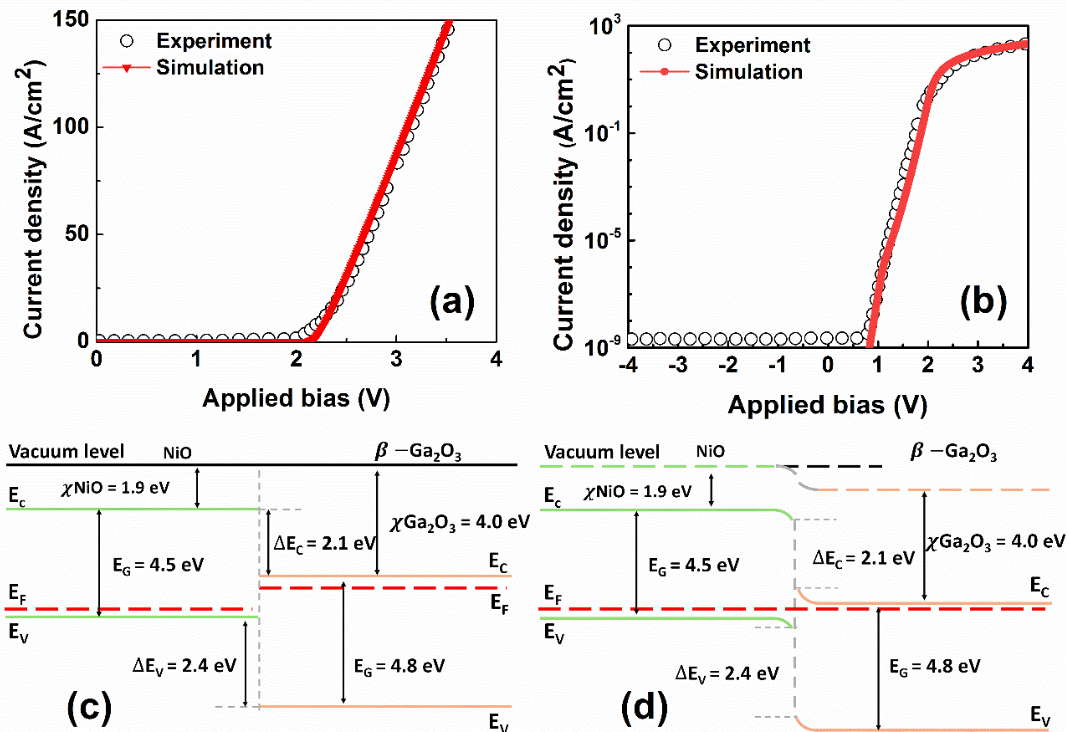

Figure 2. *I-V characteristics of NiO/β-Ga_2O_3 p-n junction diode illustrated in linear-scale (a) and log-scale (b). Schematic band diagram of NiO/Ga_2O_3 structure before (c) and after (d) the formation of NiO/Ga_2O_3 p-n junction.*

TCAD parameters are calibrated against experimental p-type NiO/n-type Ga_2O_3 diodes. The I-V characteristics, which are shown in Fig. 2(a) and Fig. 2(b) for the linear-scale and log-scale, respectively, presenting that both I-V curves fit well with the experimental reports [25]. The calibrated parameters found out in this study and shown in Table 1 are in reasonably good agreement with those reported in previous studies [15], [24].

The band diagram of the p-type NiO/n-type Ga_2O_3 p-n junction is demonstrated in Fig. 2(c) and (d). Before the formation of the p-n junction, the conduction band (CB) offset of this p-n junction is 2.1 eV. A depletion region is formed clearly after the p-n junction is created, building a CB offset of 2.1 eV and a valance band (VB) offset of 2.4 eV. The values of CB and VB offsets are in consistent with the literatures [24].

To investigate the p-type NiO/n-type Ga_2O_3 E-mode MOSFETs, the recessed-gate structure shown in Fig. 3(a) with the channel thickness of 60 nm is examined. First, the electrical properties of this MOSFETs are investigated as a function of the gate-drain distances L_{GD}. The values of L_{GD} are varied in a range from 1 to 8 µm with the step of 1 µm. All the parameters are kept in constant including the thickness of channel (60 nm) in a recessed-gate region and the doping concentration $N_A = 1.0\times10^{18}$ cm^{-3} for NiO layer and $N_D = 7.0\times10^{17}$ cm^{-3} for Ga_2O_3 layer. The thickness of Al_2O_3 is designed to be 20 nm as shown in Fig. 3(a). Fig. 3(b) shows the distribution of electric field along the cut-line from gate metal to NiO substrate shown in Fig. 3(a). The electric field is found to be highest at n-type Ga_2O_3/p-type NiO

interface. Figure 3(c) shows the I_D-V_G characteristics of p-type NiO/n-type Ga_2O_3 MOSFETs as a function of gate-drain distance L_{DG}. The drain current is found to be sensitive to the change of L_{GD}, increasing 3 times from 0.17 mA/mm to 0.57 mA/mm when L_{GD} decreases from 8 µm to 1 µm under the drain-source voltage of 3 V and the gate voltage of 2.0 V. The I_D-V_D characteristics shown in Fig. 3(d) confirms the increase of drain current as a function of L_{GD}.

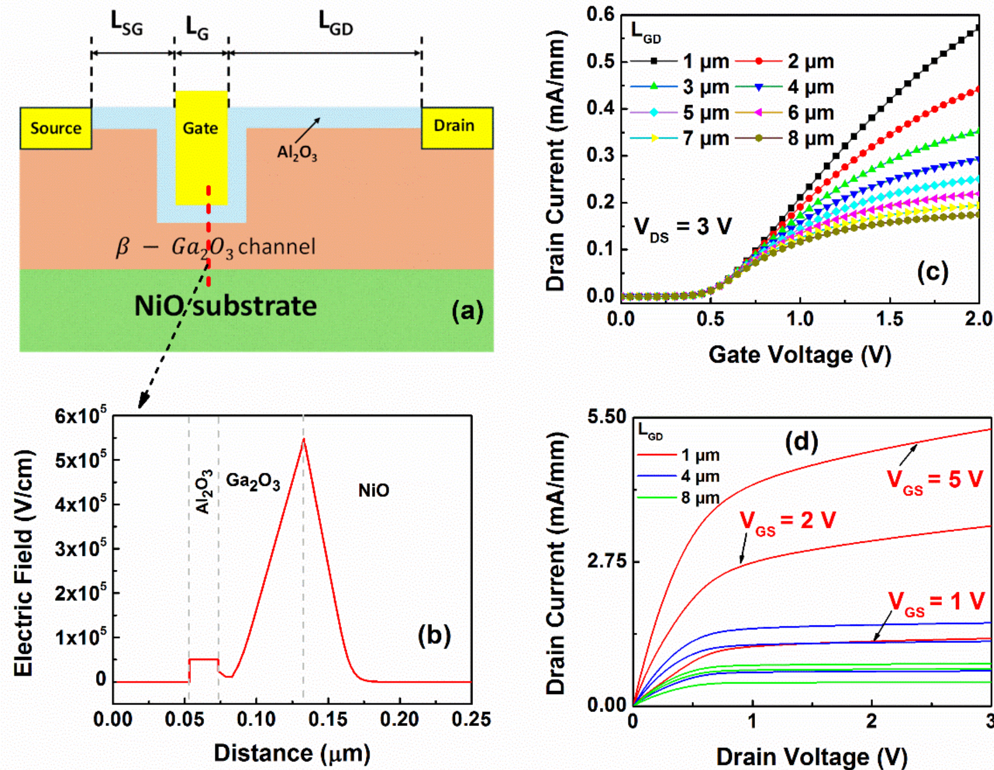

Figure 3. *(a) Schematic of recessed-gate NiO/Ga_2O_3 MOSFET, (b) Distribution of electric field along the cutline from gate to substrate of recessed-gate NiO/Ga_2O_3 MOSFET. (c) and (d) I_D-V_G and I_D-V_D characteristics of NiO/Ga_2O_3 MOSFET, respectively.*

Impacts of doping concentration N_A in NiO layer on the properties of p-type NiO/n-type Ga_2O_3 MOSFETs are illustrated in Fig. 4. It is found that drain current decrease 2 times when N_A increases from 1.0×10^{16} cm^{-3} to 1.0×10^{20} cm^{-3} shown in Fig. 4(a), due to the extension of depletion width in Ga_2O_3 side. The increase of N_A shifts I_D-V_G curves to positive direction shown in Fig. 4(b), indicating that on-current can be modulated by varying the doping concentration of NiO layer. Figure 4(c) presents the effects of N_A on on-resistance of p-type NiO/n-type Ga_2O_3 MOSFETs, illustrating the increase of on-resistance as N_A of NiO layer rises. Threshold voltage (V_{th}) is an important factor to determine a device to work in E-mode or depletion mode (D-mode). The change of V_{th} as a function of N_A is shown in Fig. 4(d), indicating that p-type NiO/n-type Ga_2O_3 MOSFETs operates in E-mode when the acceptor concentration in NiO is larger than 1.0×10^{18} cm^{-3}.

To explain the I-V characteristics obtained in Fig. 4, band diagram of p-type NiO/n-type Ga_2O_3 MOSFET is plotted in Fig. 5(a). It is found that the acceptor concentration in NiO layer significantly affects the depletion region at NiO/Ga_2O_3 interface. The depletion width widens to Ga_2O_3 channel when N_A increases from 1×10^{16} cm^{-3} to 1×10^{20} cm^{-3}. At doping concentration N_A of 1×10^{20} cm^{-3}, depletion region covers all recessed-region. The change of depletion region is in agreement with the variation of electron concentration in Ga_2O_3 channel shown in Fig. 5(b). Fig. 5 indicates that an E-mode p-type NiO/n-type Ga_2O_3 MOSFET can be obtained by modulating the doping N_A concentration of NiO layer.

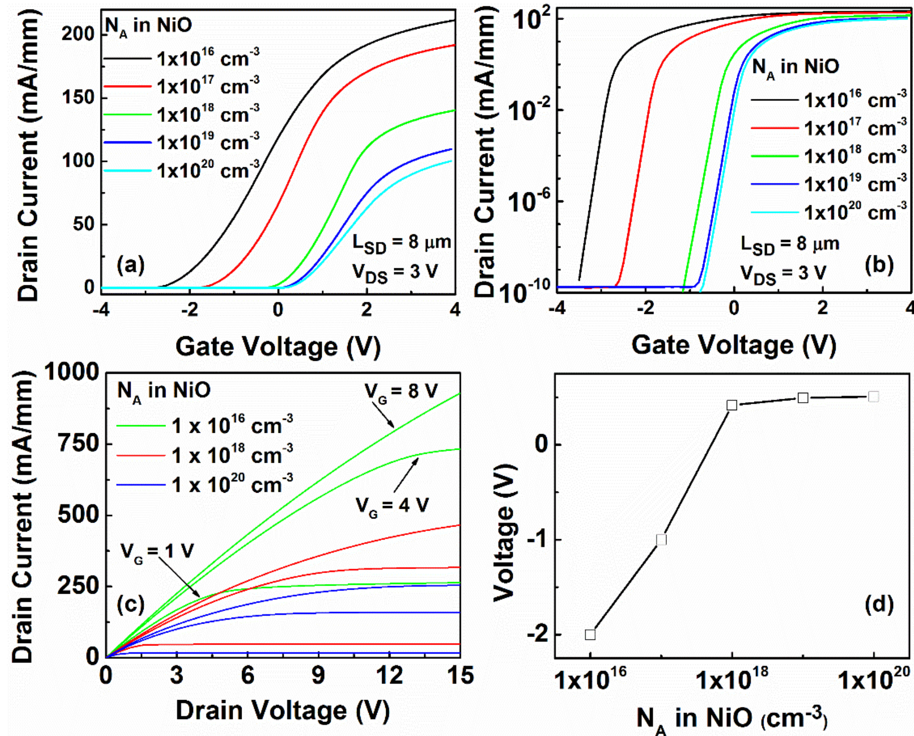

Figure 4. *I_D-V_G characteristics as a function of acceptor concentration N_A in NiO layer of recessed-gate NiO/Ga_2O_3 MOSFETs, presented in linear scale (a) and log-scale (b). (c) I_D-V_D characteristics of recessed-gate NiO/Ga_2O_3 MOSFETs. (d) The variation of threshold voltage as a function of N_A.*

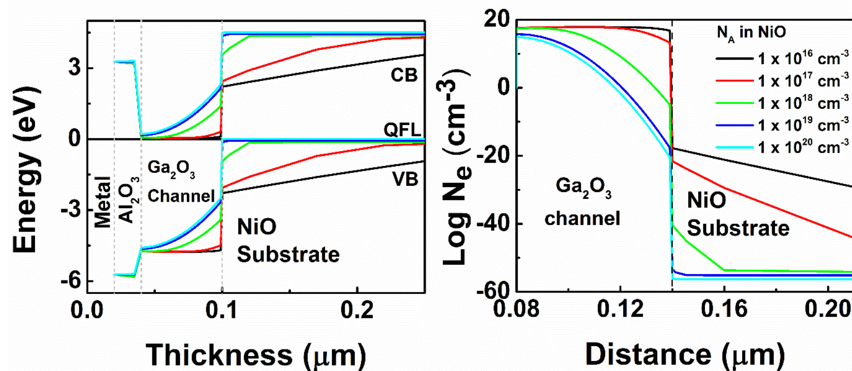

Figure 5. *(a) Band diagram of the p-type NiO/n-type Ga_2O_3 MOSFETs in unbiased condition along cut-line from gate to NiO substrate in recessed-region. (b) Distribution of electron concentration along the cut-line mentioned in Fig. 5(a).*

4. Conclusions

In conclusion, the p-type NiO/n-type Ga_2O_3 MOSFETs were investigated using TCAD simulations. The impacts of gate-drain distance of Ga_2O_3 channel layer and the acceptor concentration N_A in NiO layer on I-V characteristics of NiO/Ga_2O_3 MOSFET were conducted. It is found that drain current increases 3 times as the L_{GD} decreases in a range from 8 µm to 1 µm. Additionally, the threshold voltage (V_{th}) is strongly dependent on the acceptor concentration N_A of NiO layer. When N_A is larger than 1.0×10^{18} cm^{-3} the MOSFET operates in E-mode with $V_{th} > 0$. It was found that the NiO/Ga_2O_3 junction transformed when N_A increased from 1.0×10^{16} cm^{-3} to 1.0×10^{20} cm^{-3}, changing from a linear-junction to an abrupt-junction. This transformation induces the rise in Schottky barrier within the depletion region, leading to create the E-mode of the p-type NiO/n-type Ga_2O_3 MOSFETs. The study illustrates a systematic analysis for fabricating E-mode p-type NiO/n-type Ga_2O_3 MOSFETs, showing their great promise for next-generation power electronics applications.

Acknowledgments

This work was funded by the Ho Chi Minh City University of Technology and Education, Vietnam (grant No. SV2024-44).

Conflict of Interest

The authors declare no conflict of interest.

Data Availability Statement

The data that support the findings of this study are available from the corresponding author upon reasonable request.

REFERENCES

[1] H. von Wenckstern, "Group-III Sesquioxides: Growth, Physical Properties and Devices," *Advanced Electronic Materials,* vol. 3, p. 1600350, 2017.
[2] S. J. Pearton *et al.*, "A review of Ga2O3 materials, processing, and devices," *Applied Physics Reviews,* vol. 5, 2018.
[3] J. Yang *et al.*, "Vertical geometry 33.2 A, 4.8 MW cm2 Ga2O3 field-plated Schottky rectifier arrays," *Applied Physics Letters,* vol. 114, 2019.
[4] Z. Galazka *et al.*, "Scaling-Up of Bulk β-Ga2O3 Single Crystals by the Czochralski Method," *ECS Journal of Solid State Science and Technology,* vol. 6, p. Q3007, 2017.
[5] A. Kuramata, K. Koshi, S. Watanabe, Y. Yamaoka, T. Masui, and S. Yamakoshi, "High-quality β-Ga2O3 single crystals grown by edge-defined film-fed growth," *Japanese Journal of Applied Physics,* vol. 55, p. 1202A2, 2016.
[6] F. Alema, Y. Zhang, A. Osinsky, N. Valente, A. Mauze, T. Itoh, and J. S. Speck, "Low temperature electron mobility exceeding 104 cm2/V s in MOCVD grown β-Ga2O3," *APL Materials,* vol. 7, 2019.
[7] K. Sasaki, M. Higashiwaki, A. Kuramata, T. Masui, and S. Yamakoshi, "MBE grown Ga2O3 and its power device applications," *Journal of Crystal Growth,* vol. 378, pp. 591-595, 2013.
[8] H. Murakami *et al.*, "Homoepitaxial growth of β-Ga2O3 layers by halide vapor phase epitaxy," *Applied Physics Express,* vol. 8, p. 015503, 2014.
[9] A. Bhattacharyya *et al.*, "Multi-kV class β-Ga_2O_3 MESFETs with a lateral figure of merit up to 355 MW/cm²," *IEEE Electron Device Letters,* vol. 42, pp. 1272-1275, 2021.
[10] C. Wang *et al.*, "Demonstration of the p-NiO x/n-Ga 2 O 3 heterojunction gate FETs and diodes with BV 2/R on, sp figures of merit of 0.39 GW/cm 2 and 1.38 GW/cm 2," *IEEE Electron Device Letters,* vol. 42, pp. 485-488, 2021.
[11] X. Zhou *et al.*, "Realizing high-performance β-Ga_2O_3 MOSFET by using variation of lateral doping: a TCAD study," *IEEE Transactions on Electron Devices,* vol. 68, pp. 1501-1506, 2021.
[12] H. C. Huang *et al.*, "β-Ga2O3 FinFETs with ultra-low hysteresis by plasma-free metal-assisted chemical etching," *Applied Physics Letters,* vol. 121, 2022.
[13] Z. Feng *et al.*, "Design and fabrication of field-plated normally off β-Ga2O3 MOSFET with laminated-ferroelectric charge storage gate for high power application," *Applied Physics Letters,* vol. 116, 2020.
[14] H. Yuan *et al.*, "Contact barriers modulation of graphene/β-Ga2O3 interface for high-performance Ga2O3 devices," *Applied Surface Science,* vol. 527, p. 146740, 2020.
[15] H. B. Do, A. V. Phan-Gia, V. Q. Nguyen, and M. M. De Souza, "Optimization of normally-off β-Ga2O3 MOSFET with high Ion and BFOM: A TCAD study," *AIP Advances,* vol. 12, 2022.
[16] D. Wakimoto, C. H. Lin, Q. T. Thieu, H. Miyamoto, K. Sasaki, and A. Kuramata, "Nitrogen-doped β-Ga2O3 vertical transistors with a threshold voltage of≥ 1.3 V and a channel mobility of 100 cm2 V− 1 s− 1," *Applied Physics Express,* vol. 16, p. 036503, 2023.
[17] Y. Lv *et al.*, "Oxygen annealing impact on β-Ga2O3 MOSFETs: Improved pinch-off characteristic and output power density," *Applied Physics Letters,* vol. 117, 2020.
[18] X. Lu, Y. Deng, Y. Pei, Z. Chen, and G. Wang, "Recent advances in NiO/Ga2O3 heterojunctions for power electronics," *Journal of Semiconductors,* vol. 44, p. 061802, 2023.
[19] A. A. Ahmed, M. Devarajan, and N. Afzal, "Growth of rf sputtered nio films on different substrates—a comparative study," *Surface Review and Letters,* vol. 24, p. 1750096, 2017.
[20] Y. Wang *et al.*, "Demonstration of β-Ga_2O_3 Superjunction-Equivalent MOSFETs," *IEEE Transactions on Electron Devices,* vol. 69, pp. 2203-2209, 2022.
[21] J. S. Li *et al.*, "1 mm2, 3.6 kV, 4.8 A NiO/Ga2O3 Heterojunction Rectifiers," *ECS Journal of Solid State Science and Technology,* vol. 12, p. 085001, 2023.
[22] Y. Qin *et al.*, "10-kV Ga 2 O 3 Charge-Balance Schottky Rectifier Operational at 200° C," *IEEE Electron Device Letters,* vol. 44, pp. 1268-1271, 2023.
[23] A. K. Bhat, H. S. Kim, A. Mishra, M. D. Smith, M. J. Uren, and M. Kuball, "Analysis of interface trap induced ledge in β-Ga2O3 based MOS structures using UV-assisted capacitance–voltage measurements," *Journal of Applied Physics,* vol. 135, 2024.
[24] A. Almalki *et al.*, "Investigation of deep defects and their effects on the properties of NiO/β-Ga2O3 heterojuncion diodes," *Materials Today Electronics,* vol. 4, p. 100042, 2023.
[25] H. Gong, X. Chen, Y. Xu, F. F. Ren, S. Gu, and J. Ye, "A 1.86-kV double-layered NiO/β-Ga2O3 vertical p–n heterojunction diode," *Applied Physics Letters,* vol. 117, 2020.

Duc-Minh Truong is currently an undergraduate student in the Department of Materials Technology, Faculty of Applied Science, HCMC University of Technology and Education.
Email: 20130021@student.hcmute.edu.vn. ORCID: https://orcid.org/0009-0000-4439-6009

Ngoc-Hung Nguyen is currently a lecturer, Department of Fundamentals of Electrical Engineering, HCMC University of Technology and Education.

JTE HCMUTE
ISSN: 2615-9740
JOURNAL OF TECHNICAL EDUCATION SCIENCE
Ho Chi Minh City University of Technology and Education
Website: https://jte.edu.vn
Email: jte@hcmute.edu.vn

Email: hungnn@hcmute.edu.vn. ORCID: https://orcid.org/0009-0001-7663-8989

Huy-Binh Do received the Ph.D. degree from the National Chiao Tung University, Taiwan. He is currently a lecturer in the Department of Materials Technology, Faculty of Applied Science, HCMC University of Technology and Education.

Email: binhdh@hcmute.edu.vn. ORCID: https://orcid.org/0000-0003-3274-5050